If-less KPP

Alexander Shchepetkin, I.G.P.P. UCLA

with input from: **Xavier Capet**
François Colas
Jim Mcwilliams

San Diego, CA, October 2005

- # Why KPP?

. ...don't ask.

- ## Why if-less?

. if-switches may cause:

. discontinuities of second derivative
discontinuities of first derivative
discontinuities of function
hysteresis and **multiple** solutions

- ## To what extend if-less?

. ...identify and eliminate the most offending ones

. ...this is a data-assimilation workshop.

KPP boundary layer model:

Extent of PBL h_{bl} is determined from bulk Richardson number (LMD94)

$$Ri_b(z) = \frac{\Delta z g \left[\rho(z) - \rho_r\right] / \rho_0}{|\mathbf{u}_r - \mathbf{u}(z)|^2 + V_t^2(z)} \qquad\qquad Ri_b(-h_{\mathsf{bl}}) = \mathtt{Ri}_{\mathsf{cr}} = 0.3$$

after which h_{bl} is checked against Monin-Obukhov $h_{\mathsf{MO}} = u_*^3/\left(\kappa \cdot B_{\mathsf{f}}\right)$, and Ekman $h_{\mathsf{Ek}} = 0.7 u_*/f$ depth and limited by both of them in the case of stable buoyancy forcing $B_{\mathsf{f}} > 0$.

Once h_{bl} is known $K_{m,s}(z) = w_{m,s} \cdot h_{\mathsf{bl}} \cdot G\left(z/h_{\mathsf{bl}}\right)$ where $G(.)$ is universal non-dimensional shape function and $w_{m,s} = \kappa u_* \cdot \psi_{m,s}\left(zB_{\mathsf{f}}/u_*^3\right)$.

- relies on Monin-Obukhov similarity theory
- KPP a bulk, non-local model of intermediate complexity
- a quasi-equilibrium, diagnostic model
- multi-process model
- widely used (CCM, POP, MIT, OPA); mostly for climate modeling

Evolution of KPP: Summary of changes in KPP since 1994 by W. Large and G. Danabasoglu (2003), (2005):

- Turbulent velocity scale limit in **stable** regime
- Diurnal cycle in SW Rad. heat flux
- Critical bulk Ri depends on vertical resolution
- C_v depends on BVF
- Correct Ekman and Monin-Obukhov depth limit computations
- Compute interior convection **after** BL mixing is done
- Modify usage of N in turbulent shear computation
- Quadratic interpolation of Ri to find h_{bl}
- Monin-Obukhov depth limit is considered for elimination

Motivation

Early ROMS solution exhibit biases in thermocline depth

- too shallow in most cases

Overall excessively sensitive to numerical discretization

- h_{bl} fields are too noisy
- resolution drift: h_{bl} tends to go deeper with grid refinement

Sources of discontinuous behavior:

- $Ri_b(z)$ oscillates if $\mathbf{u}(z)$ is Ekman spiral (prevented only by h_{Ek}-limit)
- hysteresis h_{MO} limitation logic
- hysteresis h_{Ek} limitation logic
- vertical grid-point locking

Integral formulation of PBL

- $Ri_b(z)$ disregards velocity profile and 3D-nality within PBL

Calibration and tuning

- parameterization of elementary processes
- 1D experience
- 3D experience

Criterion for finding h_{bl}: We define surface PBL as an integral layer within which net production of turbulence due to shear-layer instability is balanced by dissipation due to stratification,

$$Cr(z) = \int_{z}^{\text{surface}} \mathcal{K}(z) \left\{ \left| \frac{\partial \mathbf{u}}{\partial z} \right|^2 - \frac{N^2}{\mathtt{Ri}_{\text{cr}}} - C_{\text{Ek}} \cdot f^2 \right\} dz' + \frac{V_t^2(z)}{z}$$

and search for crossing point $Cr(z) = 0$.

$N^2 = -\frac{g}{\rho_0} \cdot \frac{\partial \rho}{\partial z}\Big|_{ad}$ is B-V frequency ($ad \equiv$ adiabatic);

f is Coriolis parameter; C_{Ek} is a nondimensional constant;

$V_t^2(z)$ is unresolved turbulent velocity shear (same as in LMD94);

Integration Kernel $\mathcal{K}(z) = \frac{\zeta - z}{\epsilon h_{\text{bl}} + \zeta - z}$ is to ignore contribution from near-surface sublayer ϵh_{bl} where M-O similarity law is not valid (plays the same role as to distinguish between ρ_{ref} vs. ρ_{surf} in Ri_b of LMD94). ζ is free surface; $\epsilon = 0.1$.

- Same result as Ri_b the case of linear velocity profile, but otherwise

$$\int_{z'}^{z''} \left|\frac{\partial \mathbf{u}}{\partial z}\right|^2 dz \geq \frac{\left|\mathbf{u}'' - \mathbf{u}'\right|^2}{z'' - z'}$$

- $Cr(z)$ is **monotonic** for Ekman spiral $\Rightarrow$ no sudden jumps of h_{bl}

- Numerically more attractive, since $\mathbf{u}(z)$ and $\rho(z)$ can be reconstructed as continuous functions

- Avoids introduction of *reference* potential density: basically integration Brunt-Väisäla frequency. Allows formalism of *adiabatic* derivatives and differences to achieve monotonicity

- Correct account for thermobaric effect: Bill Large: to determine extent of BL one must bring water parcel **from reference depth to** $z = -h_{\mathrm{bl}}$ and compare its density with the ambient fluid **there**. We never did it this way in ROMS community (?)

- Avoids ambiguity for merging top and bottom BLs

Pure physical limits:

destabilizing vs. stabilizing effects:

- balance $\left|\frac{\partial \mathbf{u}}{\partial z}\right|^2$ vs. $\frac{N^2}{\mathtt{Ri}_{\mathsf{cr}}}$ $\Rightarrow$ shear layer instability

- $\left|\frac{\partial \mathbf{u}}{\partial z}\right|^2$ vs. $C_{\mathsf{Ek}} \cdot f^2$ $\Rightarrow$ turbulent Ekman layer

- *negatively* forced $\frac{N^2}{\mathtt{Ri}_{\mathsf{cr}}}$ vs. V_t^2 $\Rightarrow$ free convection

Monin-Obukhov depth limit $h_{\text{bl}} \le h_{\text{MO}} = \dfrac{C^{\text{MO}} \cdot u_*^3}{\kappa \cdot B_{\text{f}}}$ if $B_{\text{f}}(z) > 0$.

Because of solar radiation absorption, buoyancy forcing $B_{\text{f}} = B_{\text{f}}(z)$ increases with depth, possibly changing sign *from unstable to stable* $\Rightarrow$ a case when $B_{\text{f}}\,(-\text{overestimated } h_{\text{bl}}) > 0$, but $B_{\text{f}}\,(-h_{\text{MO}}) < 0 \Rightarrow$ **hysteresis** and oscillations in h_{bl}

solution # 1: (2003) use $B_{\text{f}} = B_{\text{f}}\,(-h_{\text{MO}})$ in computation of h_{MO}, i.e. implicit search for k enclosing z^*, such that

$$z_k \le z^* \le z_{k+1} \qquad \text{and} \qquad h_{\text{MO}}\,(z_k) \le |z^*| \le h_{\text{MO}}\,(z_{k+1})$$

then solve
$$\frac{h_{\text{MO}k}\,(z_{k+1} - z^*) + h_{\text{MO}k+1}\,(z^* - z_k)}{z_{k+1} - z_k} + z^* = 0$$

resulting in
$$h_{\text{MO}} = -z^* = \frac{\frac{C^{\text{MO}} u_*^3}{\kappa}\left(B_{\text{f}}{}'_{k+1} z_{k+1} - B_{\text{f}}{}'_k z_k\right)}{B_{\text{f}}{}'_{k+1} B_{\text{f}}{}'_k\,(z_{k+1} - z_k) + \frac{C^{\text{MO}} u_*^3}{\kappa}\left(B_{\text{f}}{}'_k - B_{\text{f}}{}'_{k+1}\right)}$$

above $B_{\text{f}}{}' = \max\,(B_{\text{f}}, 0)$; if k not found $\Rightarrow$ no limit; **no singularity** if either $B_{\text{f}} \to 0$; limit applied **outside** $B_{\text{f}} > 0$ **logic**: it is already taken into account in computing h_{MO}; **since h_{bl} is not involved $\Rightarrow$ no possibility of hysteresis**

solution # 2: (2005) Eliminate M-O limit altogether.

Ekman depth limitation: $h_{\text{bl}} \leq h_{\text{Ek}} = 0.7u_*/f$ for *stable* boundary layer; should be $h_{\text{bl}} = h_{\text{Ek}}$ for *neutral* forcing and stratification

Length $\mathcal{L} = u_*/f$ and velocity $\mathcal{U} = u_*$ are natural scaling parameters for neutrally stratified problem

$$i \cdot f\mathbf{u} = \frac{\partial}{\partial z}\left(w_m|z|\frac{\partial \mathbf{u}}{\partial z}\right)$$

where $\mathbf{u} = u + iv$, and $w_m \equiv \kappa u_*$, and κ is von Karman constant.

- Most vertical mixing schemes are "Coriolis-blind".
- Coriolis effect plays no role in determining h_{bl} via bulk Ri criterion; h_{Ek}-limit is applied *a'posteriori*, and only for stable buoyancy forcing.
- Because of light absorption, stability increases downward resulting in hysteresis if $B_{\text{f}}\,(\text{unlimited } h_{\text{bl}}) > 0$, but $B_{\text{f}}\,(h_{\text{Ek}}) < 0$ which is manifested by h_{bl} oscillations and jumps

??? integrate h_{Ek}-limit into KPP BL criterion, balance

$$\int \left|\frac{\partial \mathbf{u}}{\partial z}\right|^2 dz' \qquad \text{vs.} \qquad \int f^2 dz' \qquad ???$$

DNS and LES simulations of Turbulent Ekman Layer:

Zikanov, O., D. N. Slinn, and M. R. Dhanak, 2003: Large-eddy simulations of the wind-induced turbulent Ekman layer. *J. Fluid. Mech.*, **495**, 343-368.

Esau, I., 2004: Simulation of Ekman Boundary Layers by Large Eddy Model with Dynamic Mixed Sub-filter Closure. *Envir. Fluid Mech.*, **4**, 273-303, DOI: 10.1023/B:EFMC.0000024236.38450.8d

Coleman G. N., 1999: Similarity statistics from direct numerical simulation of the neutrally stratified PBL. *J. Atmos. Sci.*, **56**, 891-900.

Coleman G. N., J. H. Ferziger, and P. R. Spalart, 1990: A numerical study of the turbulent Ekman layer. *J. Fluid. Mech.*, **213**, 313-348.

Parmhed, O., I. Kos, and B.Grisogono, 2005: An improved Ekman layer approximation for smooth eddy diffusivity profiles. *Boundary-Layer Meteor.*, 115(3), 399-407.

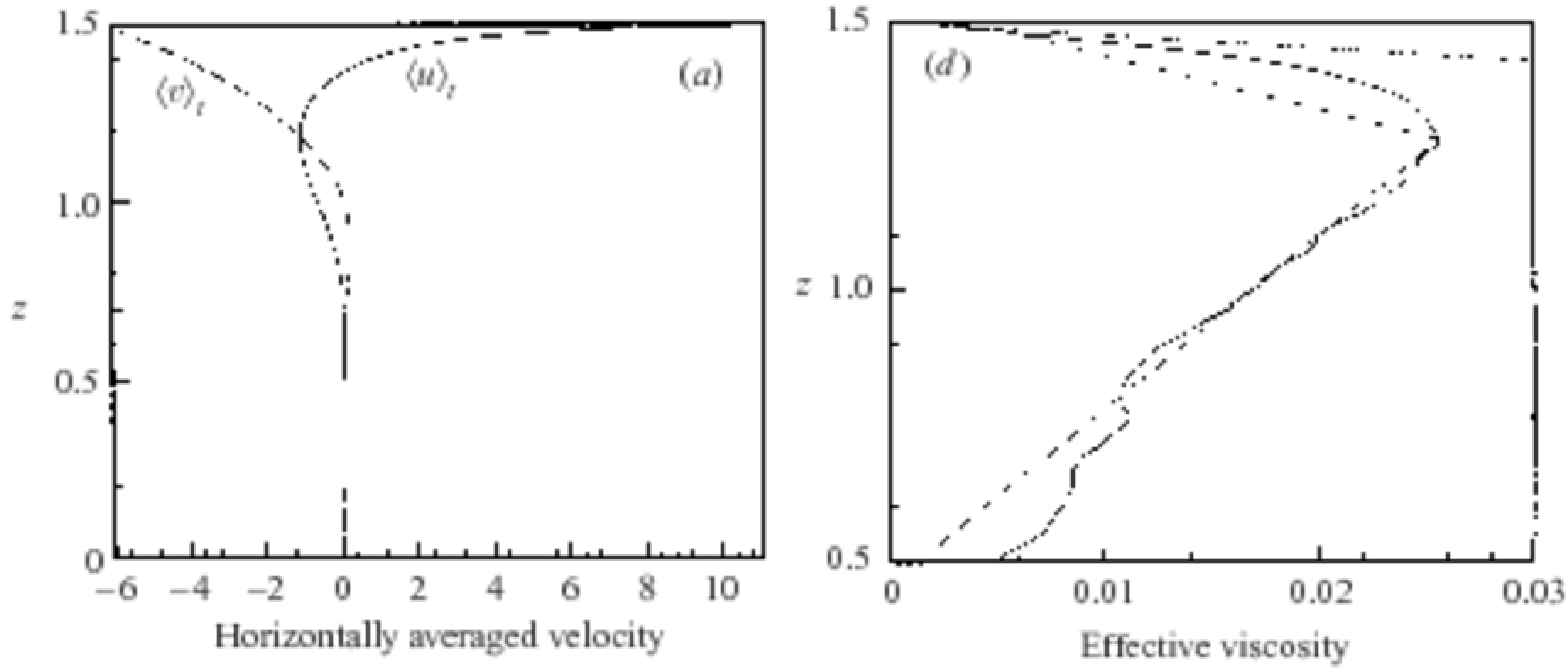

DNS simulations from, Zikanov *et al 2003*.

Modified Ekman problem: $$i \cdot f\mathbf{u} = \frac{\partial}{\partial z}\left[w_m \mathcal{L} G\left(\frac{z}{\mathcal{L}}\right)\frac{\partial \mathbf{u}}{\partial z}\right]$$

G is KPP non-dimensional shape function

$$G(\sigma) = |\sigma|\,(1-\sigma)^2 + \begin{cases} \frac{(\sigma-\sigma_0)^2}{2\sigma_0}, & \sigma < \sigma_0 \\ 0 & \text{otherwise} \end{cases} \qquad \sigma_0 = 0.1$$

B.C.: $$w_m \mathcal{L} G\left(\frac{z}{\mathcal{L}}\right)\left.\frac{\partial \mathbf{u}}{\partial z}\right|_{z=0} = u_*^2 \mathbf{1}_\tau \quad \Rightarrow \quad \left.\frac{\partial \mathbf{u}}{\partial z}\right|_{z=0} = \frac{u_* \mathbf{1}_\tau}{\kappa \mathcal{L}\sigma_0/2}$$

$\mathbf{u} = 0$, if $z < -\mathcal{L}$

Nondimensionalization: Postulate that depth of generated this way boundary layer is equal to Ekman length and introduce scaling,

$$z = \mathcal{L}\sigma = \sigma \cdot 0.7 u_*/f \qquad \mathbf{u} = u_* \cdot \tilde{\mathbf{u}}\,,$$

hence

$$\frac{\partial}{\partial \sigma}\left(G(\sigma)\frac{\partial \tilde{\mathbf{u}}}{\partial \sigma}\right) = i \cdot \frac{\kappa}{0.7}\tilde{\mathbf{u}}\,, \qquad \left.\frac{\partial \tilde{\mathbf{u}}}{\partial \sigma}\right|_{\sigma=0} = \frac{2}{\kappa\sigma_0}\,, \qquad \tilde{\mathbf{u}}\Big|_{\sigma<-1} = 0$$

everything has been scaled out.

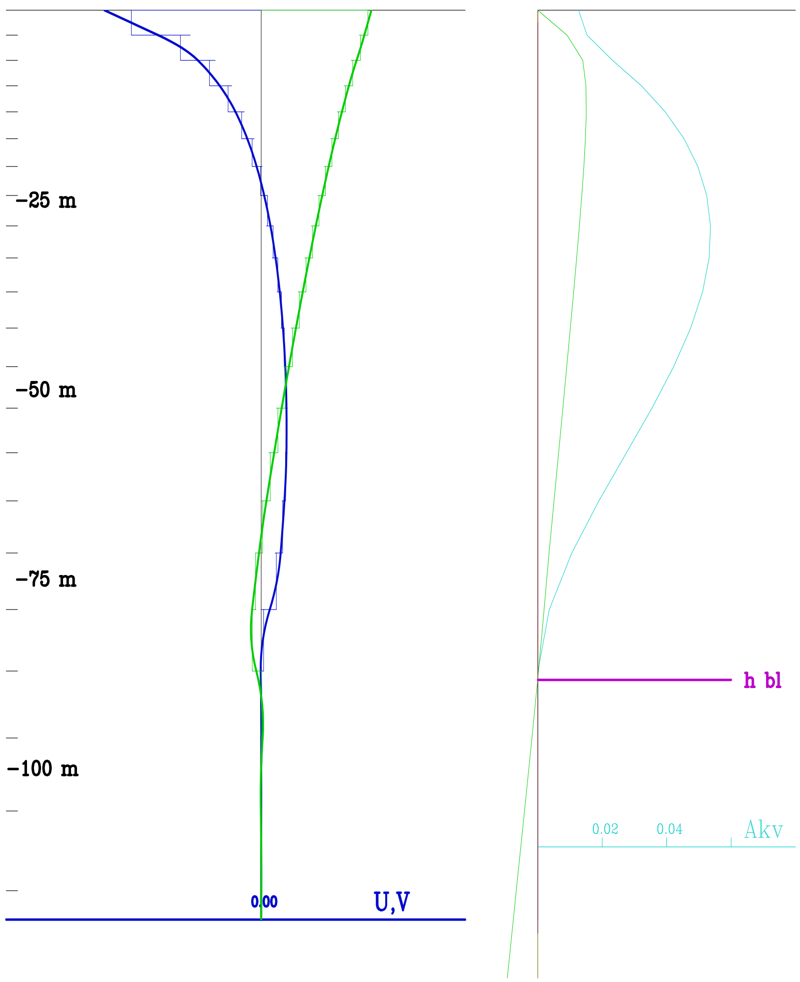

Recognize Coriolis force as *stabilizing* effect (balancing vertical shear production), construct

$$Cr(z) = \int_z^{\text{surf}} \mathcal{K}\left(z'\right)\left\{\left|\frac{\partial \mathbf{u}}{\partial z}\right|^2 - C_{\text{Ek}} \cdot f^2\right\} dz'$$

apply the same scaling

$$\widetilde{Cr}(\sigma) = \frac{1}{(0.7)^2}\int_\sigma^0 \mathcal{K}(\sigma)\left\{\left|\frac{\partial \tilde{\mathbf{u}}}{\partial \sigma}\right|^2 - C_{\text{Ek}}\right\} d\sigma'$$

and demand that $\widetilde{Cr}(-1) = 0$.

$C_{\text{Ek}} = 258$ provided that

$\mathcal{K}(\sigma) = |\sigma|/(|\sigma| + \epsilon)$, where $\epsilon = 0.1$

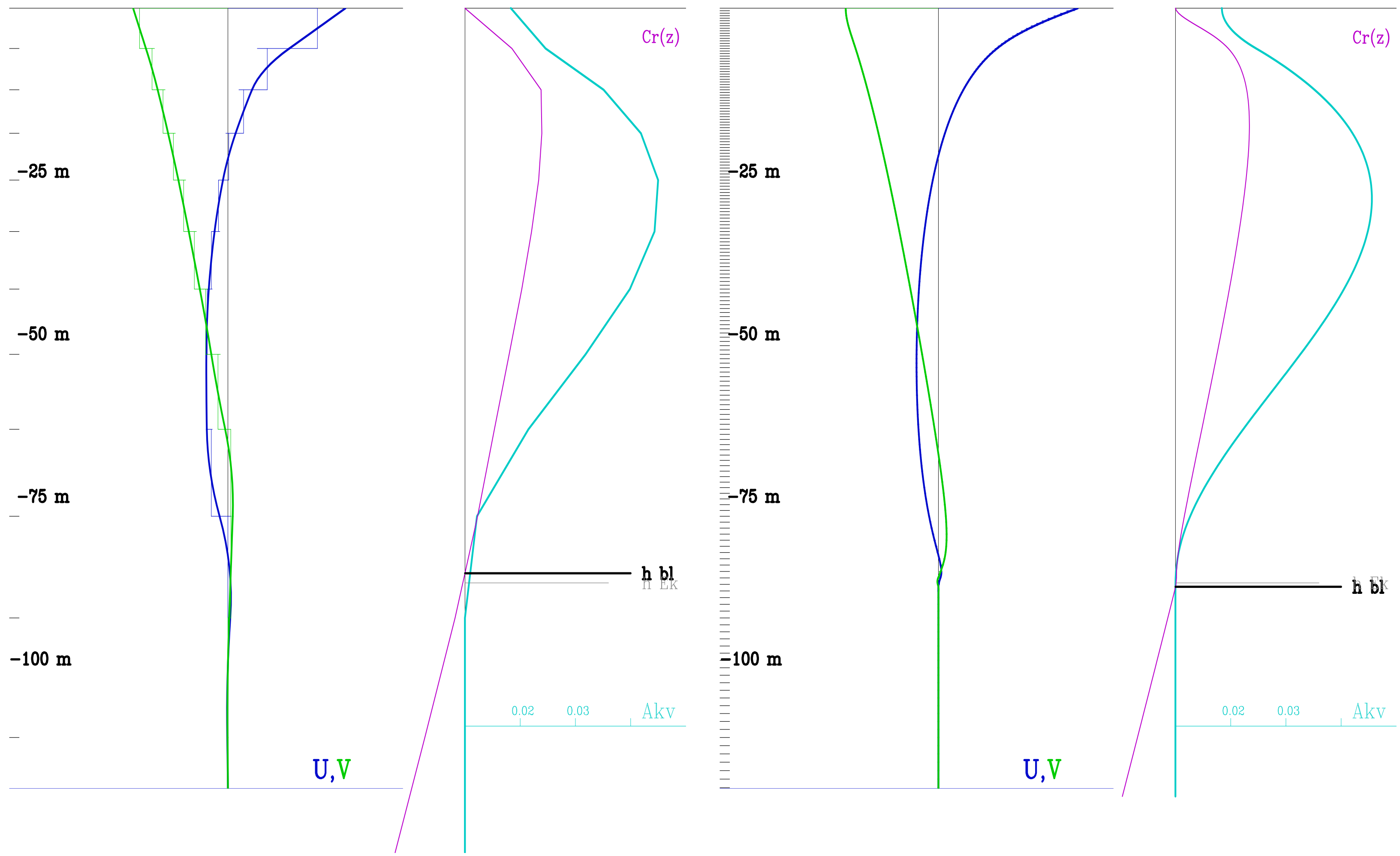

.

Coarse, $N = 32$ and fine, $N = 512$ resolution. h_{Ek} is shown for reference only and does not participate in determining h_{bl}.

- **presence of $\mathcal{K}(\sigma)$ is essential for convergence**
- **overall extremely robust**

Numerical Issues

velocities are smooth across $z = -h_{\text{bl}}$, **but tracers are not**

Computation of Ri_b/Cr at vertical ρ vs. W-points:

- ρ-placement is natural for finite-difference (trapezoidal-rule) terms in Ri_b/Cr (but not for V_t^2), however

$$A_{k+1/2} \sim \left(z_{k+1/2} - |h_{\text{bl}}|\right)^2$$

  near the edge of PBL, hence needs h_{bl} needs accuracy relatively to W-points, while missing ρ-s is more forgiving

- Estimate V_t^2 and $Cr(z)$ at midpoints $z_{k+1/2}$ using monotonized fit for bouyoncy (integrated N^2) to estimate its values and derivates at $z_{k+1/2}$-interfaces.

- *harmonic* averaging of *adiabatic* differences of density field (the same idea as for computing horizontal pressure gradient)

⇒ unlocking vertical steppiness

⇒ larger variation of PBL, typically shallower in summer

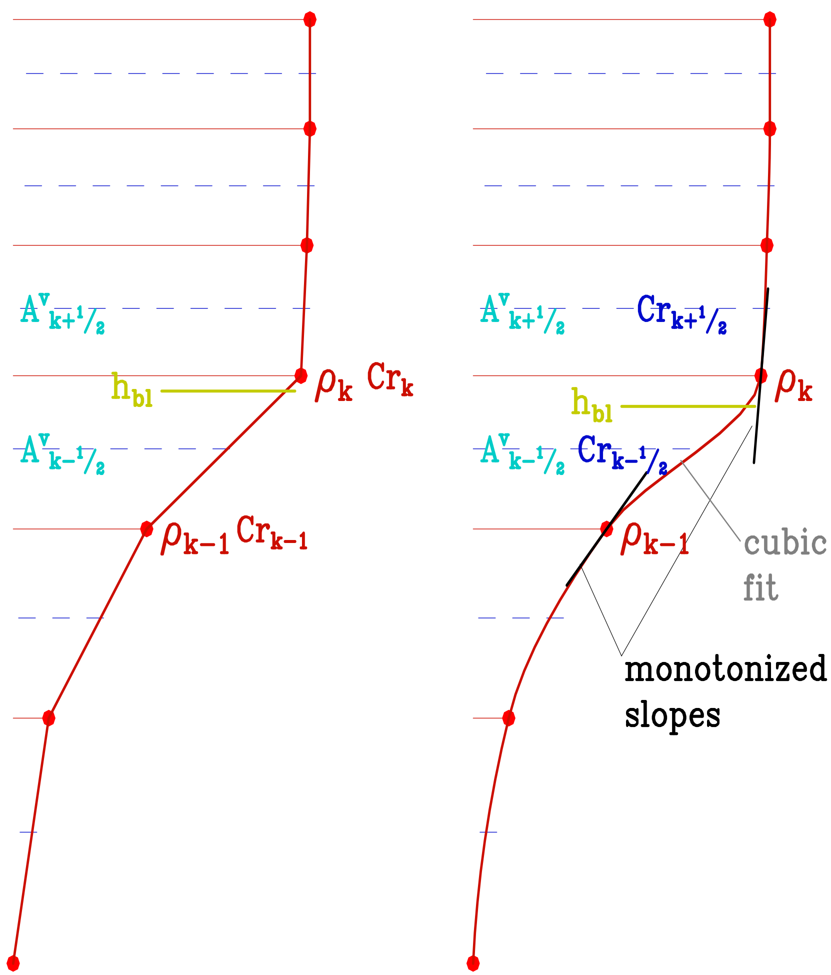

Monotonized reconstruction to compute ${V_t^2}_{k+1/2}$ and $\rho_{k+1/2}$, but **not** to interpolate Cr to find h_{bl}: because of

$$Cr \sim w_s\sqrt{N^2 - N^2 d}$$

$Cr(z)$ is **not monotonic** near

$$z = -h_{\mathsf{bl}}$$

even if $\rho(z)$ and $u, v(z)$ are

$\Rightarrow$ quadratic (cubic) interpolation for Cr is dangerous

Overall this is by far the largest cause of numerical sensitivities in KPP.

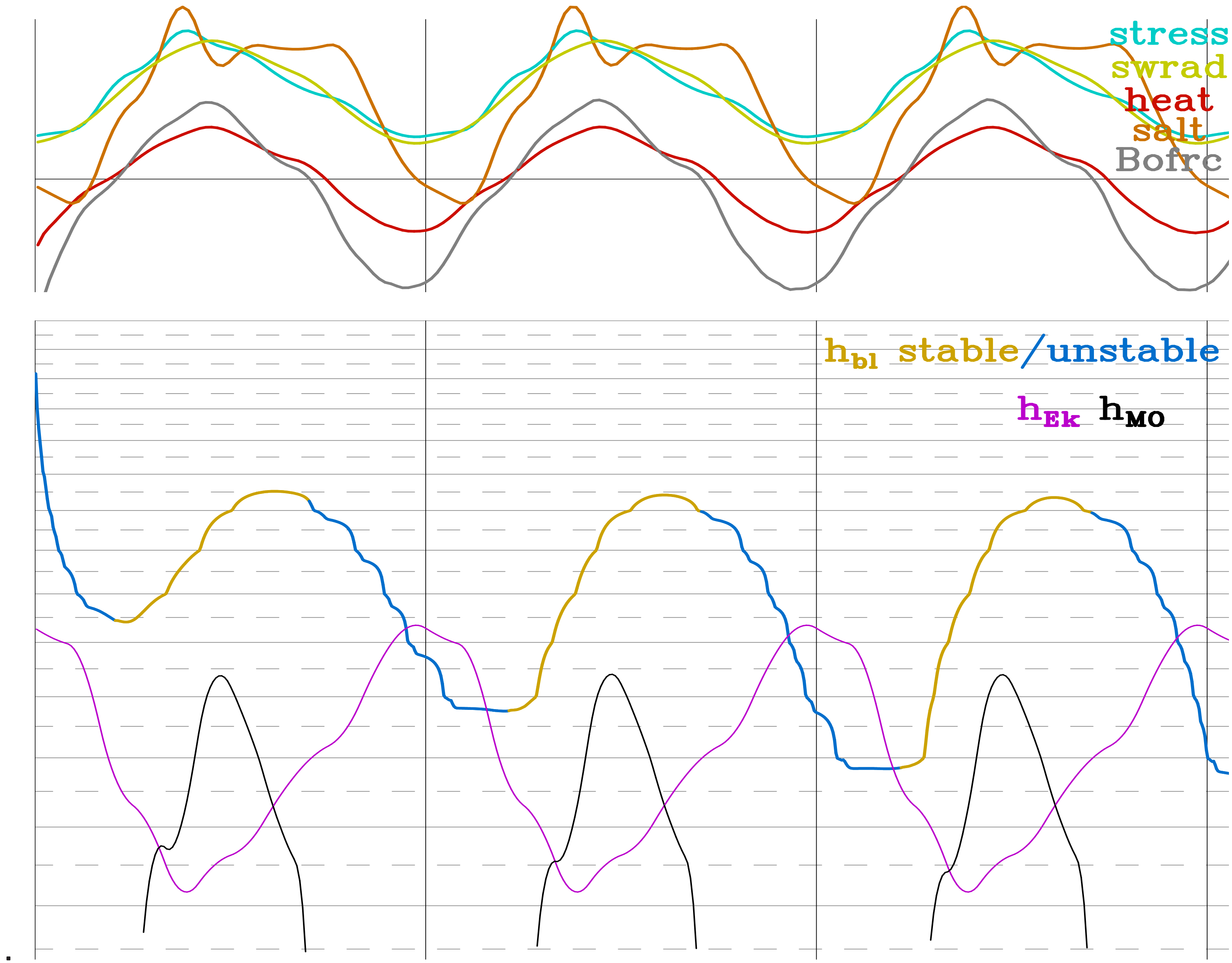

$Cr(z)$ at W-points, $N = 40$

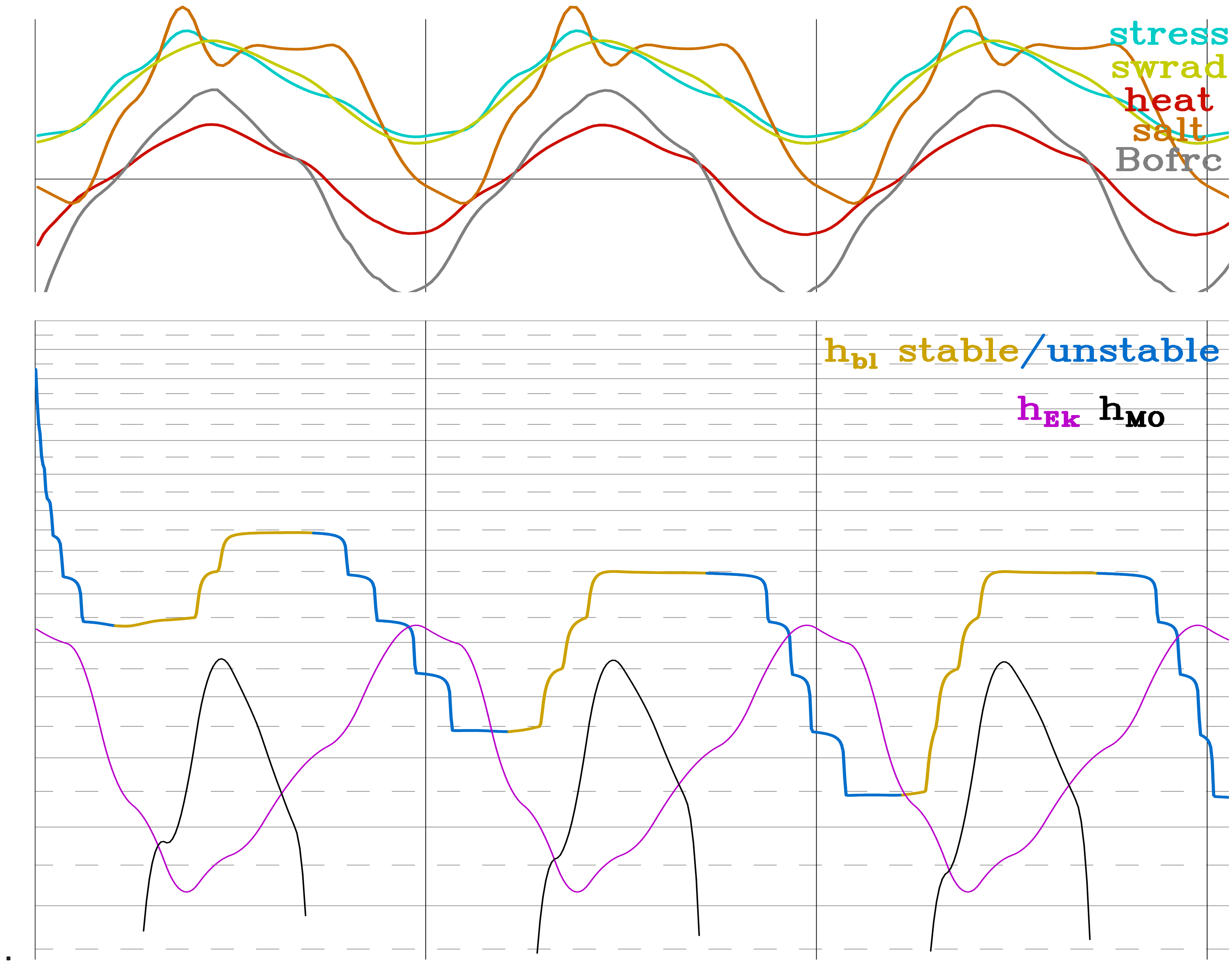

$Cr(z)$ at ρ-points, $N = 40 \Rightarrow$ grid locking

What it all adds up to?

- 1D
- 3D
- comparison with reality

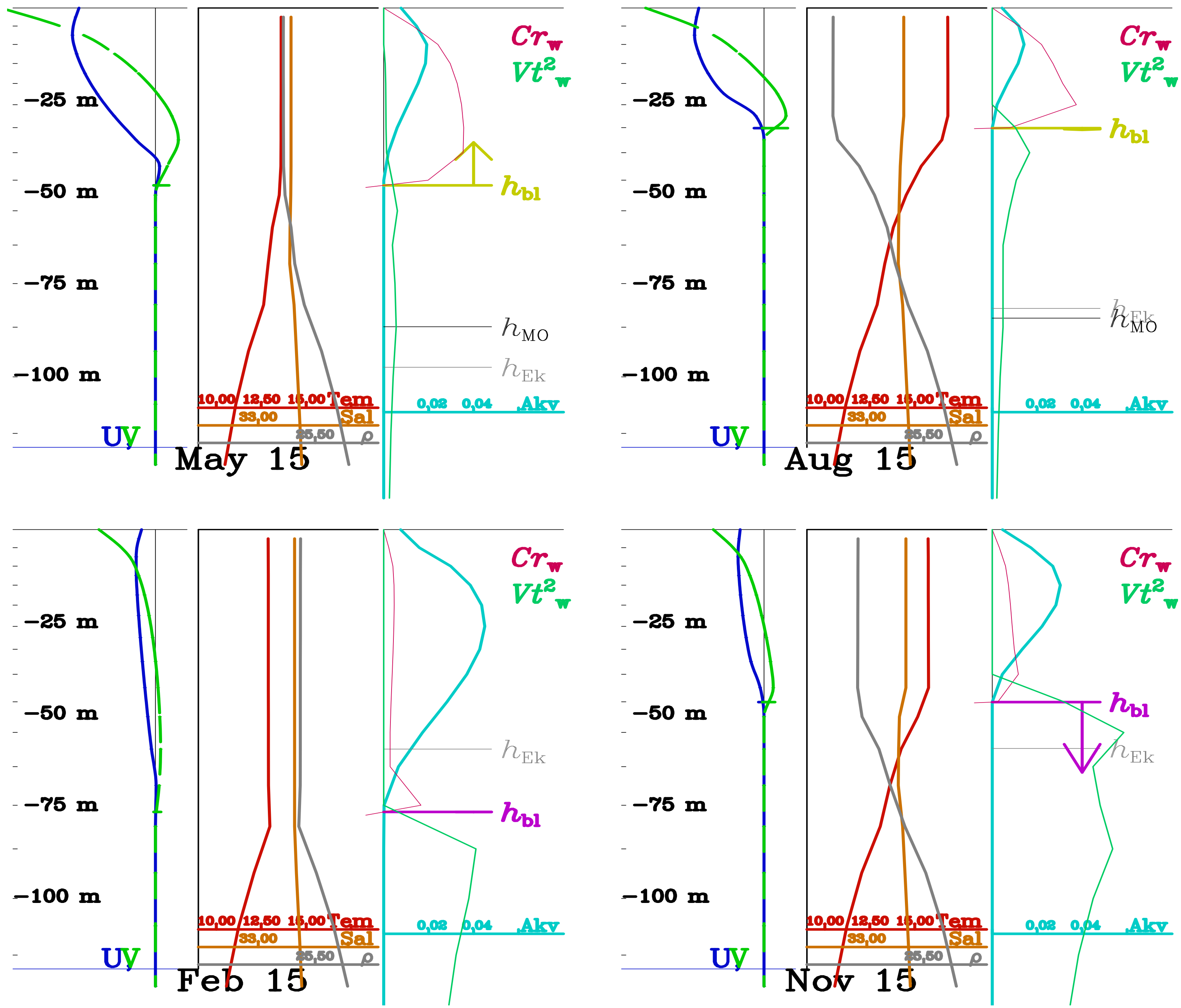

−25 m
−50 m
−75 m
−100 m
UV
10,00 12,50 15,00 Tem
33,00 Sal
25,50 ρ
0,02 0,04 Akv
Cr_w
Vt²_w
h_bl
h_MO
h_Ek
May 15
Aug 15
Feb 15
Nov 15

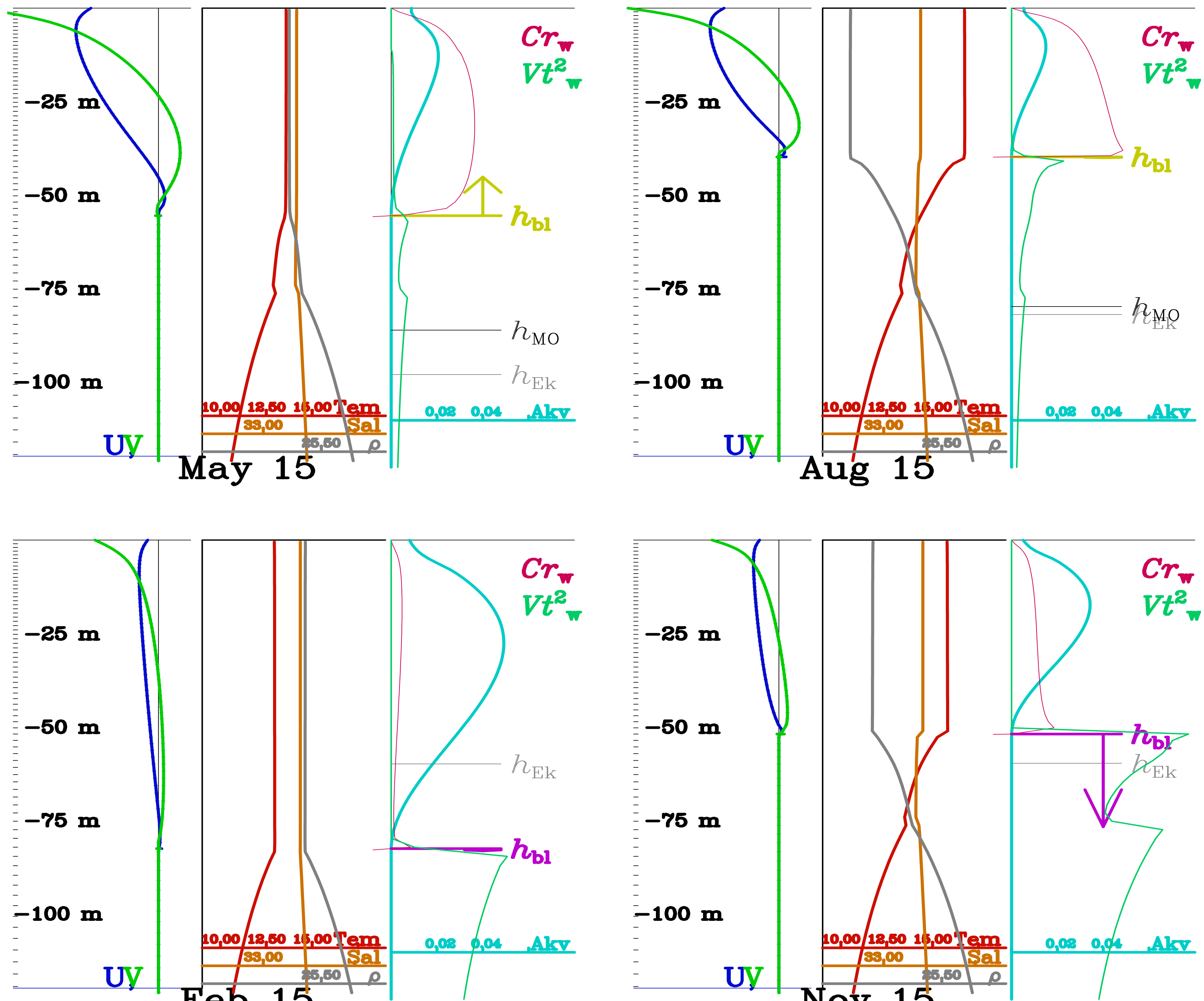

−25 m
−50 m
−75 m
−100 m
UV
10,00 12,50 15,00 Tem
33,00 Sal
25,50 ρ
0,02 0,04 Akv
Crw
Vt2w
hbl
hMO
hEk
May 15
Aug 15
Feb 15
Nov 15

3D Modeling

0.45-degree Pacific Model forced by NCEP winds

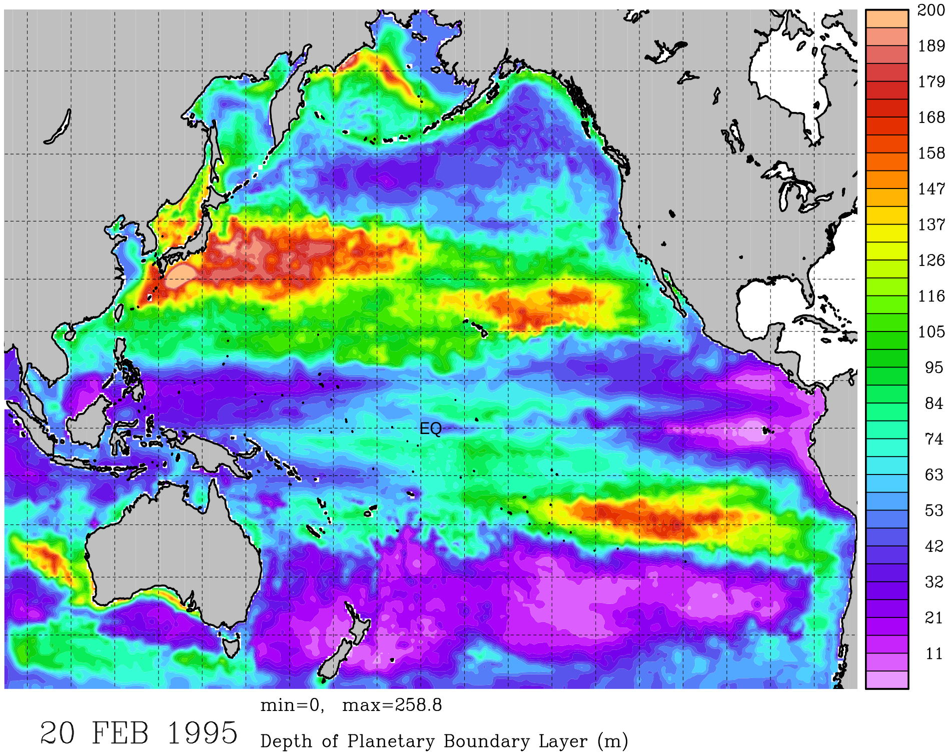

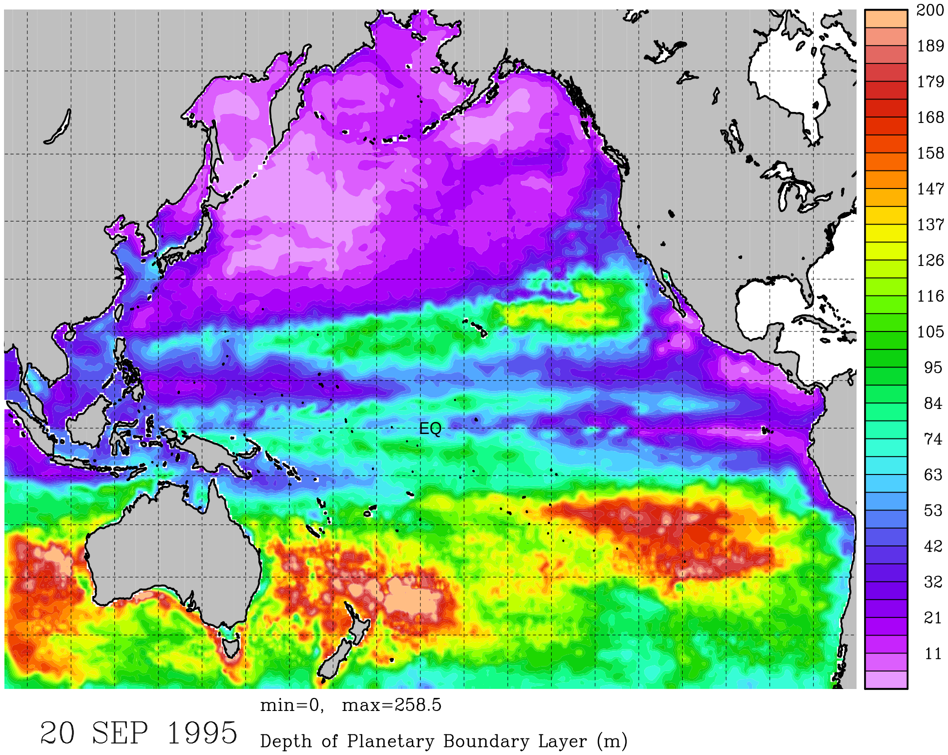

seasonal variation of h_{bl}-field

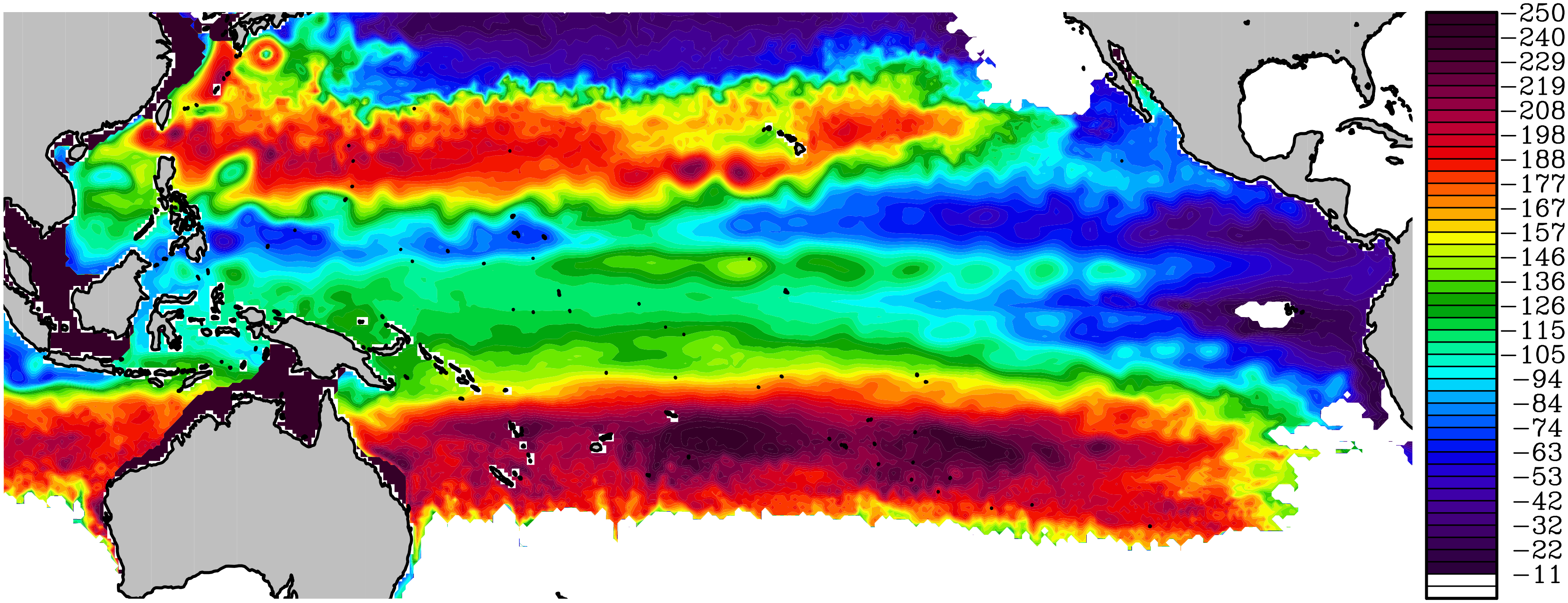

Depth of 20^0C isoterm, instantaneous snapshot from a recent 2005 simulation

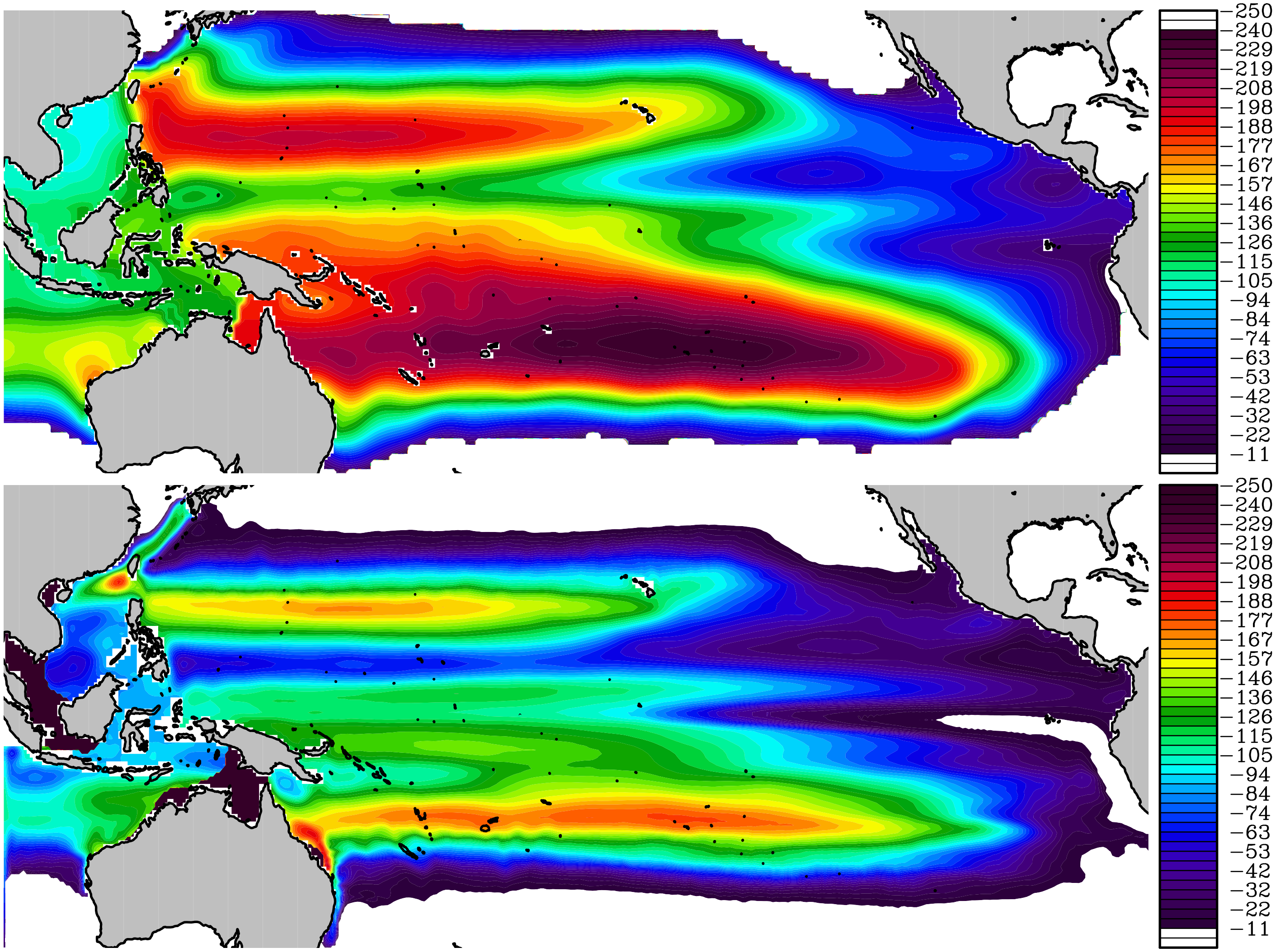

Depth of 20^0C isoterm, 10-year annual mean

Levitus

vs.

ROMS with early 2003 *baseline* KPP

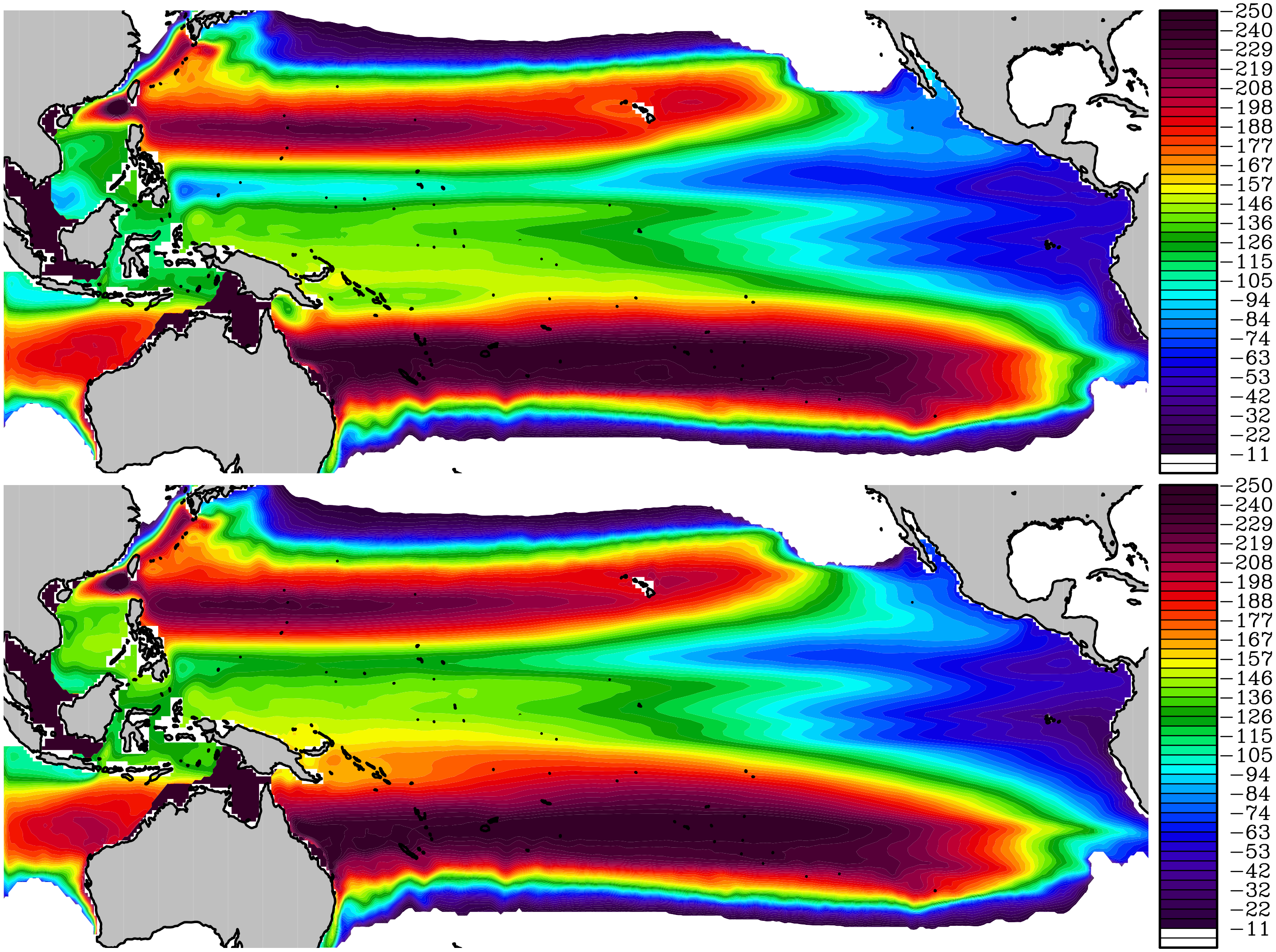

NCEP

vs.

ERS winds

New KPP in both, $Ri_{cr} = 0.45$

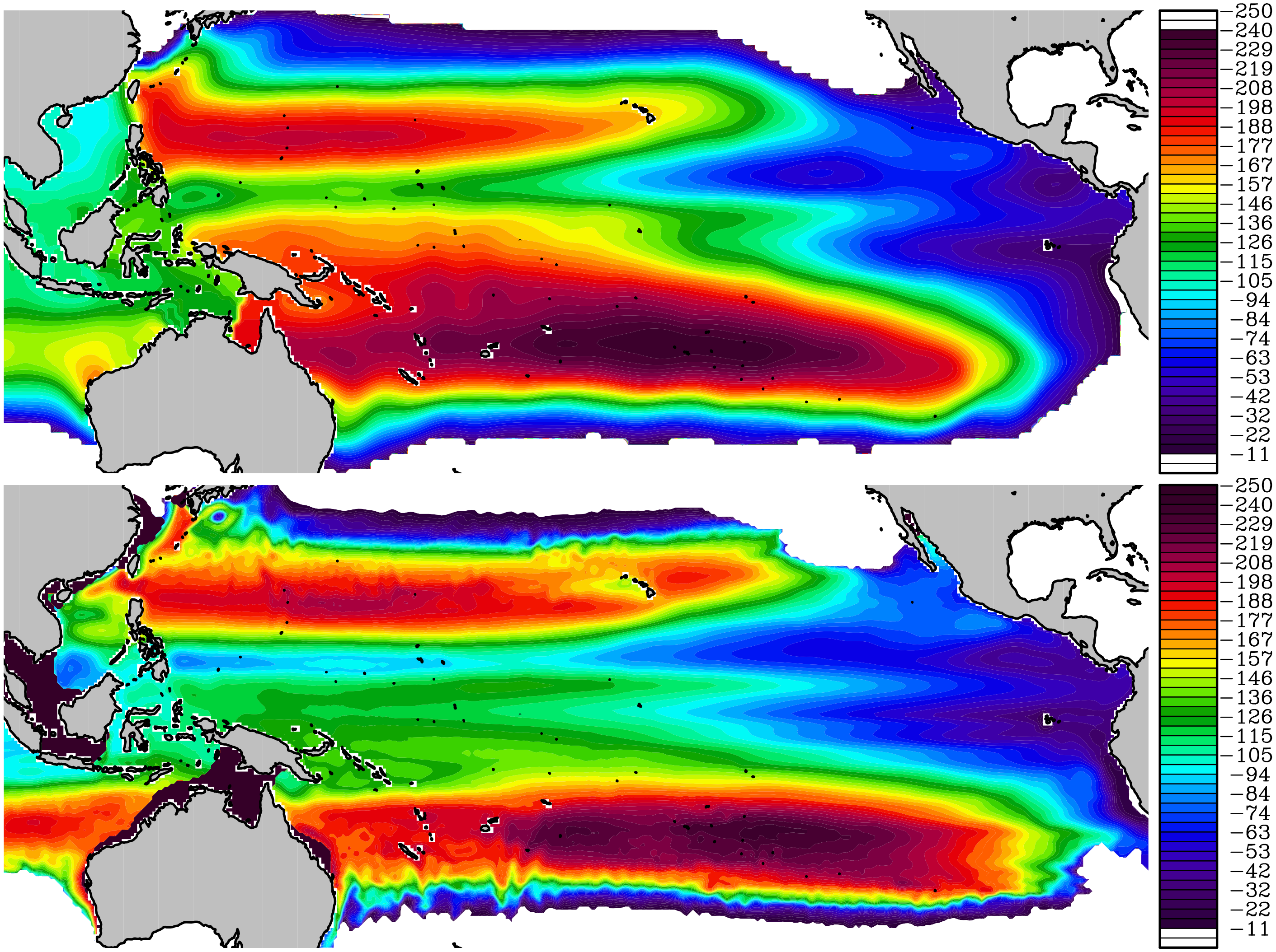

Levitus

vs.

ROMS
with 2005
KPP
still NCEP

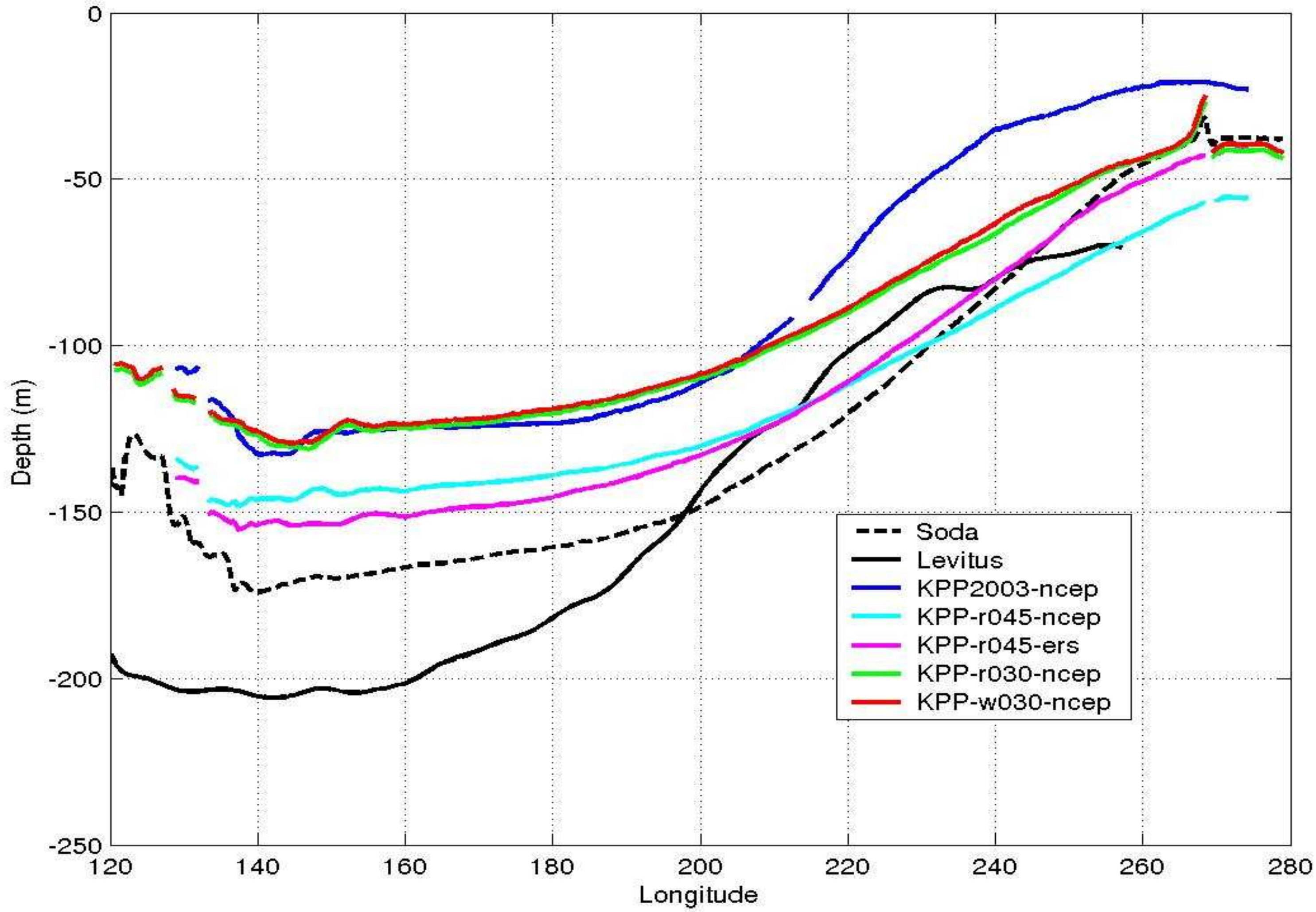

0
-50
-100
-150
-200
-250
Depth (m)
120
140
160
180
200
220
240
260
280
Longitude
Soda
Levitus
KPP2003-ncep
KPP-r045-ncep
KPP-r045-ers
KPP-r030-ncep
KPP-w030-ncep

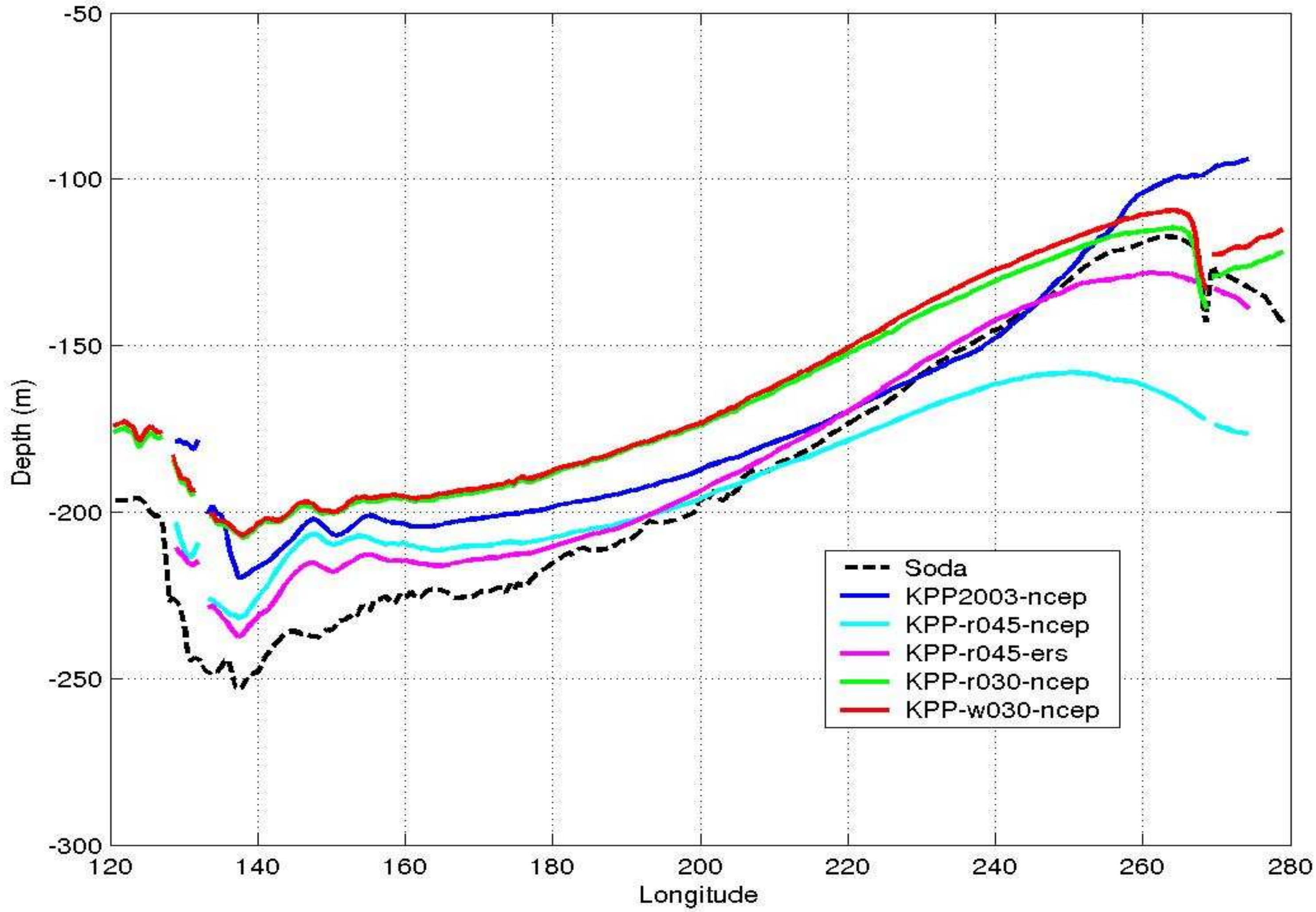

-50
-100
-150
-200
-250
-300
Depth (m)
120
140
160
180
200
220
240
260
280
Longitude
Soda
KPP2003-ncep
KPP-r045-ncep
KPP-r045-ers
KPP-r030-ncep
KPP-w030-ncep

US West Coast Model: an Example of Fine Tuning

US West Coast Model, 15 km resolution forced by COAMPS daily winds

All conditions below are the same, except variations in KPP code.

CalCOFFI (nearshore, $< 250\,km$), and Levitus (beyond that)

showing only summer because this is the worst among 4 seasons

courtesy of Xavier Capet

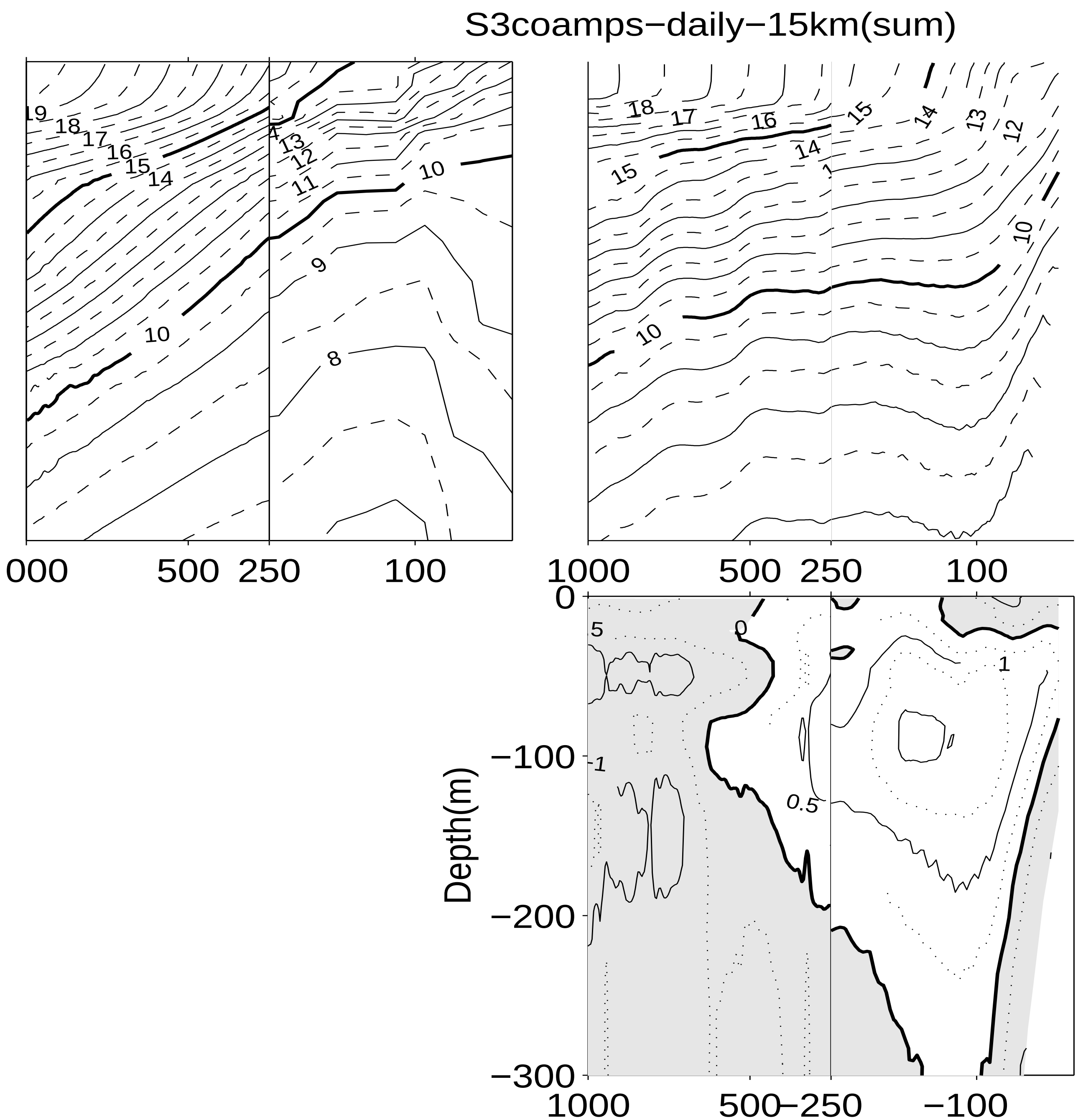

Early 2005 KPP, $\mathtt{Ri}_{cr} = 0.45$, limiting d/L_{MO} for $w_{m,s}$ in stable regime

Note slope of $10^{O}C$- isoterm

overall $1.5^{O}C$ cold bias offshore and $> 2^{O}C$ warm bias nearshore

S3coamps−shallow−15km(sum)

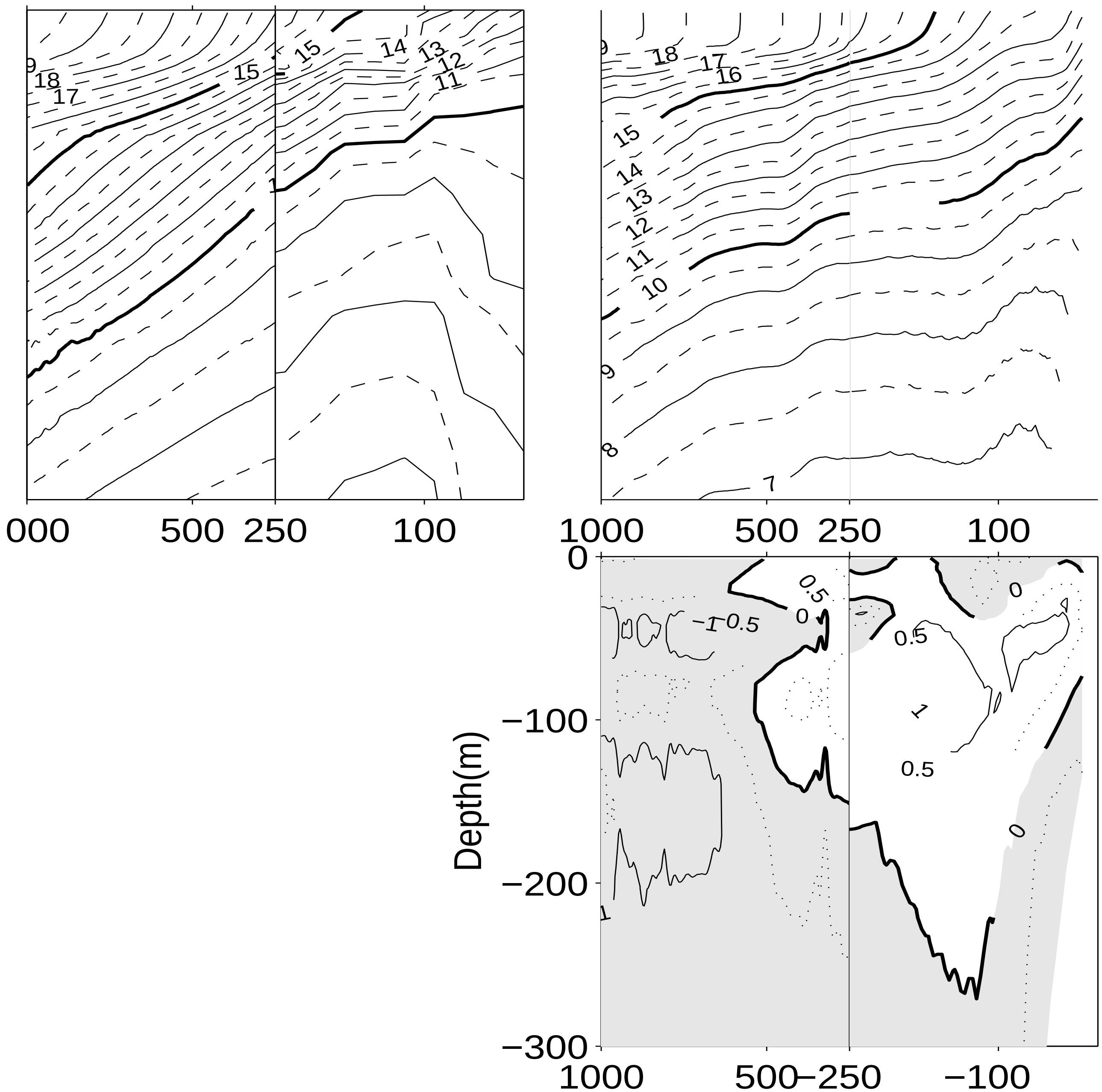

New 2005 KPP

$\mathtt{Ri}_{\mathrm{cr}} = 0.45$

Not limiting d/L_{MO}
in stable regime

(Fig. 2 of LMD94)

recovered most of the slope

S3coamps−daily$_n$kkpr−luo−15km(sum)

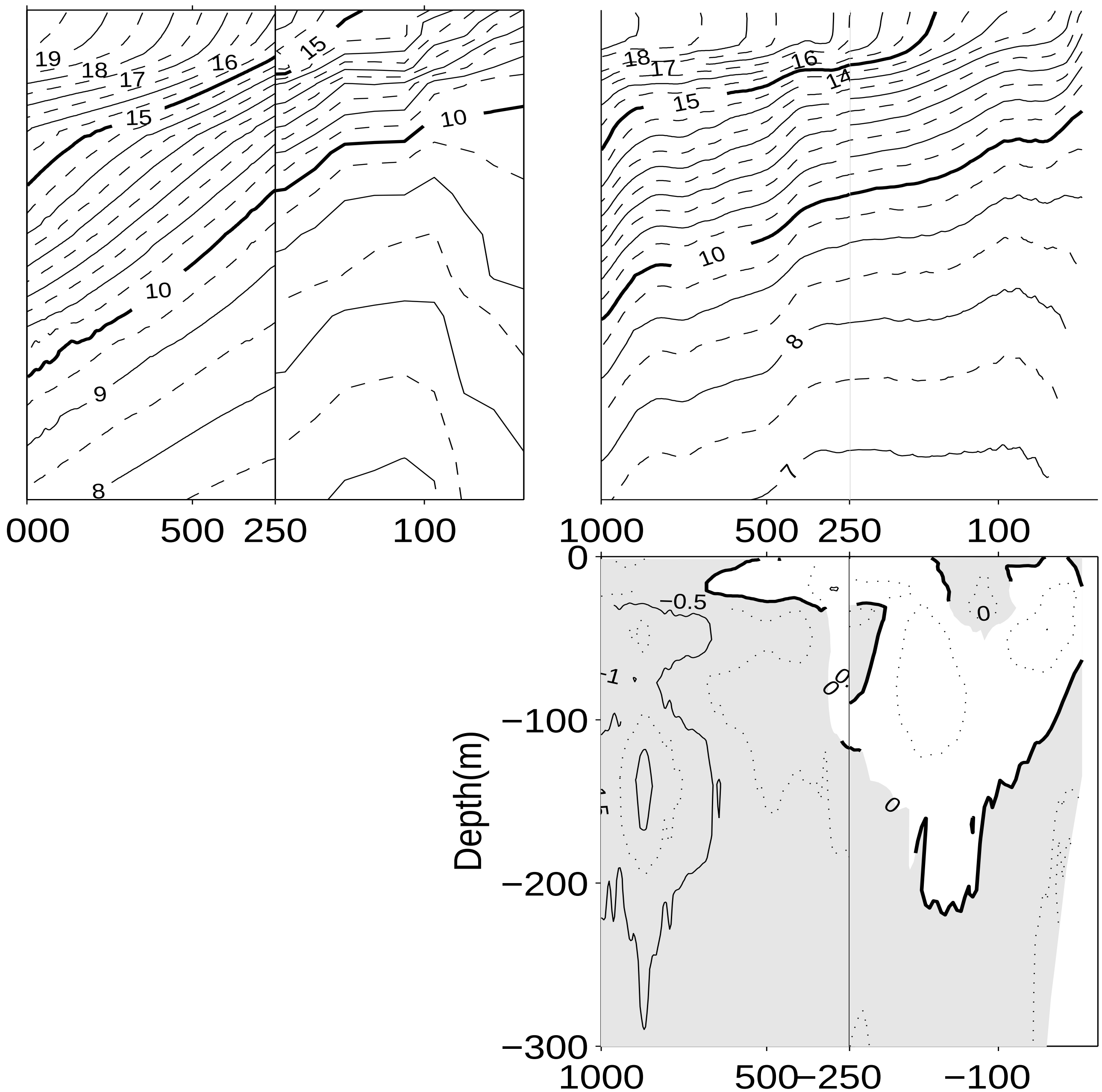

$\mathtt{Ri}_{cr} = 0.3$
No d/L_{MO} limit

shallow bias off-shore

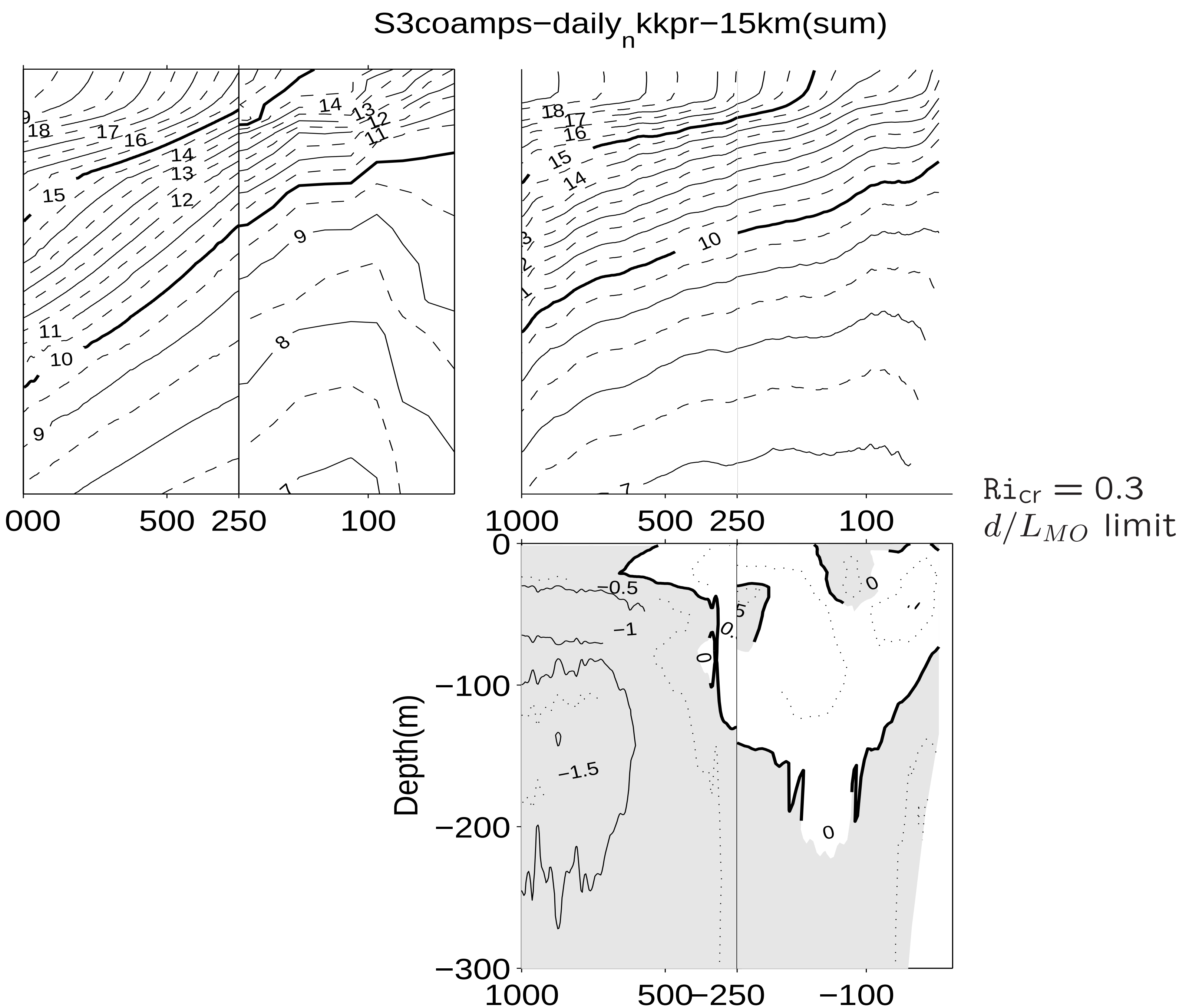

S3coamps−daily_nkkpr−15km(sum)
Ri_cr = 0.3
d/L_MO limit
Depth(m)
000
500
250
100
1000
0
−100
−200
−300
−0.5
−1
−1.5
10

Summary

- Accepted most (not all) updates from W. Large and G. Danabasoglu
- **integral Cr-based search for h_{bl}**
- kernel $\mathcal{K}(\sigma)$ to account for surface sublayer $\Rightarrow$ convergence
- replaced h_{Ek} limit with new treatment of Ekman boundary layer
- Corrected Monin-Obukhov limitation algorithm.
  Subsequently eliminated it altogether
- Do not limit $\zeta = d/L_{MO}$ in $w_{m,s}$ computation in stable regime
- Changed non-local flux to ensure its continuity at h_{bl}
- Surface wave mixing: $A_k \rightarrow$ finite limit at $z \rightarrow \zeta$
- **Significantly reduced resolution drift**
- **"shallow bias" is now under control**
- Changes for free-surface compatibility with free surface of ROMS
  (fixed blow-ups in shallow regions)
- code rewritten from scratch (yet, again) for efficiency

Lessons learned

- 1D model is very useful for process studies and numerical algorithm verification, but **not for parameter tuning against real-world data**
- Boundary layer depth h_{bl}, is it diagnosed by KPP, is not directly comparable to mixed layer empirically derived from data (cf., Levitus, $0.8^{O}C$-rule, etc). Compare primary field [T,S] field structure instead.
- 3D simulations show significantly less sensitivity to KPP algorithm and parameter settings than 1D, yet the quantitatively the differences are comparable to that of different forcing products